

Article ID: 1006-8775(2019) 03-0336-08

## TESTING DRAG COEFFICIENT APPROACHES BY USING THE BUOY DATA COLLECTED IN MODERATE TO HIGH WIND UNDER FOLLOWING, CROSSING AND OPPOSING SWELL CONDITIONS

PENG Wen-wu (彭文武)<sup>1</sup>, GAO Zhi-qiu (高志球)<sup>2</sup>, LI Yu-bin (李煜斌)<sup>2</sup>, ZHANG Rong-zhi (张荣智)<sup>3</sup>,  
TONG Bing (童兵)<sup>1</sup>, WU Bin-gui (吴彬贵)<sup>4</sup>, HE Yi-jun (何宜军)<sup>5</sup>

(1. Jiangsu Key Laboratory of Agriculture Meteorology, School of Applied Meteorology, Nanjing University of Information Science and Technology, Nanjing 210044 China; 2. School of Atmospheric Physics, Nanjing University of Information Science and Technology, Nanjing 210044 China; 3. Meteorological Center of East China Regional Air Traffic Management Bureau of Civil Aviation of China, Shanghai 201105 China; 4. Tianjin Institute of Meteorological Science, Tianjin 300074 China; 5. Collaborative Innovation Center on Forecast and Evaluation of Meteorological Disasters, School of Oceanography, Nanjing University of Information Science and Technology, Nanjing 210044 China)

**Abstract:** Hurricane intensity and track are strongly affected by air-sea interactions. Classified as following swells, crossing swells, and opposing swells, the observed wave height was parameterized by using the 10-m wind speed collected on 5 buoys by the National Buoy Data Center during 13 hurricane events. The path information of these 13 hurricanes was obtained from the National Hurricane Center Best Track (NHC-BT). Results show that the wave height increases exponentially with the 10-m wind speed, and the wave height reaches the maximum value, 11.2 m (8.1 m), when 10-m wind speed is 40 m s<sup>-1</sup> under the following and crossing (opposing) swell conditions. We find that the wave steepness (the ratio of wave height to wave length) is proportional to the -2/3 power of the wave age (the ratio of wave phase velocity to 10-m wind speed). The parameterizations of friction velocity and drag coefficient are tested using the buoy data collected in moderate to high wind under following, crossing and opposing swell conditions. A wave age dependent equation for drag coefficient is found more accurate and recommended for future usage in numerical models. Furthermore, these algorithms also suggest that wind-swell orientation needs to be considered to retrieve accurate surface drag under high winds and strong swells.

**Key words:** drag coefficient; high wind; wave height; wave age; swell

**CLC number:** P404      **Document code:** A

doi: 10.16555/j.1006-8775.2019.03.005

### 1 INTRODUCTION

Quantitative understanding of air-sea interactions in tropical cyclone environment is of great importance to the development of storm forecasting models (e.g., Green and Zhang<sup>[1, 2]</sup>). Tropical cyclone simulations are especially sensitive to the exchange of both heat and momentum between the atmosphere and ocean surface (Ooyama<sup>[3]</sup>; Emanuel<sup>[4]</sup>; Rogers et al.<sup>[5]</sup>; Soloviev et al.<sup>[6]</sup>; Peng and Li<sup>[7]</sup>; Ming and Zhang<sup>[8]</sup>). The ratio of exchange coefficient of enthalpy ( $C_K$ , the exchange coefficients of heat and water vapor, which is assumed to be equal) to drag coefficient ( $C_D$ ) is related to the maximum storm intensity

and the developing time scale of tropical cyclones, and ranges from 0.75 to 1.5 in the high wind region of intense storms (Emanuel<sup>[4]</sup>; French et al.<sup>[9]</sup>).  $C_K$  is less sensitive to wind speed (Jeong et al.<sup>[10]</sup>), while  $C_D$  does not continue to increase at higher wind speeds (Donelan et al.<sup>[11]</sup>; Bi et al.<sup>[12]</sup>). There has been an increasing interest in developing parameterizations for  $C_D$  under hurricane conditions in the last 20 years. Recently, Green and Zhang<sup>[2]</sup> proposed an empirical quadratic equation to parameterize  $C_D$  from the 10-m wind speed. Peng and Li<sup>[7]</sup> showed that previous studies obtained different relationships between  $C_D$  and  $U_{10}$  (wind speed at 10 m height), and they attributed the discrepancy among previous results to extensive wave-breaking processes and to different observed behaviors of individual fields and laboratory waves in high wind conditions. Peng and Li<sup>[7]</sup> therefore proposed a parabolic model of the drag coefficient, Equation (1), for storm surge simulation in the South China Sea and found that it outperforms traditional linear models.

$$C_D = -a(U_{10} - 33)^2 + c. \quad (1)$$

However, it is difficult to interpret the physics behind Equation (1). So far, the parameterization of sea surface  $C_D$  in high wind conditions has not reached a

**Received** 2018-08-14; **Revised** 2018-06-04; **Accepted** 2019-08-15

**Foundation items:** National Key Projects of Ministry of Science and Technology of China (2018YFC1506405); National Natural Science Foundation of China (41475014, 41675018, 41675009, 41711530223)

**Biography:** GAO Zhi-qiu, Professor, primarily undertaking research on land-sea-atmosphere interaction.

**Corresponding author:** GAO Zhi-qiu, e-mail: zgao@nust.edu.cn

general agreement among the scientific community (Anctil and Donelan<sup>[13]</sup>; Zachry et al.<sup>[14]</sup>).

Field observations have shown large scatter in  $C_D$  especially under high wind condition (Bi et al.<sup>[12]</sup>). It is argued that this large scatter is caused by the spatial and time variation in the wave field (Peng and Li<sup>[7]</sup>). Previous work (e.g., Donelan et al.<sup>[15]</sup>; Yelland and Taylor<sup>[16]</sup>; Oost et al.<sup>[17]</sup>; Oost and Oost<sup>[18]</sup>; Gao et al.<sup>[19]</sup>; Donelan et al.<sup>[20]</sup>) demonstrated that  $C_D$  over the sea surface depends not only on wind speed but also on wave state in moderate wind conditions. Using measurements from the Humidity Exchange over the Sea Main Experiment (HEXMAX), Gao et al.<sup>[21]</sup> proposed a set of dependence relationships of friction velocity ( $u_*$ ) and neutral drag coefficient ( $C_{DN}$ ) to wave age ( $c_p U_{10}^{-1}$ ) and non-dimensional significant wave height ( $gH_s U_{10}^{-2}$ ) (Gao et al.<sup>[22]</sup>). As an extension, based on buoy data collected during 13 hurricane events, the present study attempts to extend these dependence relationships to high wind condition.

## 2 BUOY DATA AND HURRICANE TRACK DATA

The buoy data and the hurricane track data used here are, respectively, from National Buoy Data Center (NDBC) (<http://www.ndbc.noaa.gov>) and National Hurricane Center (NHC) (<http://www.nhc.noaa.gov/>) of

US National Oceanic and Atmospheric Administration (NOAA). The NDBC website provides detailed descriptions of the observational instruments and the hourly meteorological and wave data. These data are quality controlled by NDBC (see NDBC Technical Document 09-02: Handbook of Automated Data Quality Control Checks and Procedures) and are widely used. Five buoys (42001, 42002, 41048, 42056, and 42057) which collected surface data during 13 hurricanes are selected in present work (Fig. 1 and Table 1). The data within 1500 km of the hurricanes center are used here, and the observed 10-m wind speeds for the 13 hurricanes all exceeded 20 m s<sup>-1</sup> on these buoys. Buoys 42001, 42002, 41048, and 42057 are 3-m discus buoys that measure wind speed at 5-m height. Buoy 42056 is a 3-m foam buoy that measures wind speed at 4-m height. Wind speeds from the historical yearly NDBC buoy records are collected at the anemometer height and need to be adjusted to be wind speeds at 10-m height for our purpose, since it is conventional to use the 10-m wind speed for studying air-sea interactions. The temporal interval of hurricane track data is 6 hours. Hurricane tracks with different colors differentiating the hurricanes and the buoy positions are shown in Fig. 1. Table 1 shows the geographical locations of the buoys, the water depths and each hurricane's name and year.

**Table 1.** Buoy geographical locations, water depths and hurricane name (year).

Buoy Number	Latitude(°N)	Longitude(°W)	Water Depth(m)	Observed Hurricane Name (year)
42001	25.9	89.667	3246	Allen (1980), Danny (1985), Opal (1995), Isidore (2002), Katrina (2005), Ike (2008), Lili (2002), Rita (2005)
42002	25.167	94.413	3566	Ike (2008), Jerry (1989)
41048	31.978	69.649	5261	Kyle (2008)
42056	19.874	85.059	4446	Emily (2005), Wilma (2005), Dean (2007)
42057	17.60	80.75	293	Wilma (2005)

Black et al.<sup>[23]</sup> defined three azimuthal sectors with three different types of swell in the radar altimetry wave observations of hurricane Bonnie (1998). Donelan et al.<sup>[24]</sup>, Sugihara et al.<sup>[25]</sup>, and Holthuijsen et al.<sup>[26]</sup> also categorized the swell into three different types. Following these studies, swells are categorized into three types (following swell, opposing swell and crossing swell) here to analyze the combined influence of wind speed and wave orientation on turbulent transfer: following swell travels within 20°–150° from the hurricane center moving direction, opposing swell travels within 150°–240°, and crossing swell travels within 240°–20°. In Fig. 2, the hurricane center is set as the origin, while the relative position of buoys is located relative to the hurricane center, and then the observed data are categorized in to

the three types (following swell, opposing swell and crossing swell) following Black et al.<sup>[23]</sup> and Holthuijsen et al.<sup>[26]</sup>.

## 3 RESULTS AND DISCUSSION

### 3.1 Parameterizing the significant wave height using 10-m wind speed

Significant wave height ( $H_s$ ) and 10-m wind speed ( $U_{10}$ ) are independently measured at each buoy. Fig. 3 shows the relationship between  $H_s$  and  $U_{10}$ , which were collected at 5 buoys during 13 hurricane events whose tracks are shown in Fig. 1. It is evident that (1) in the following swell regime and crossing swell regime the relationships between  $H_s$  and  $U_{10}$  are very close to each other; and (2) the relationship between  $H_s$  and  $U_{10}$  for all

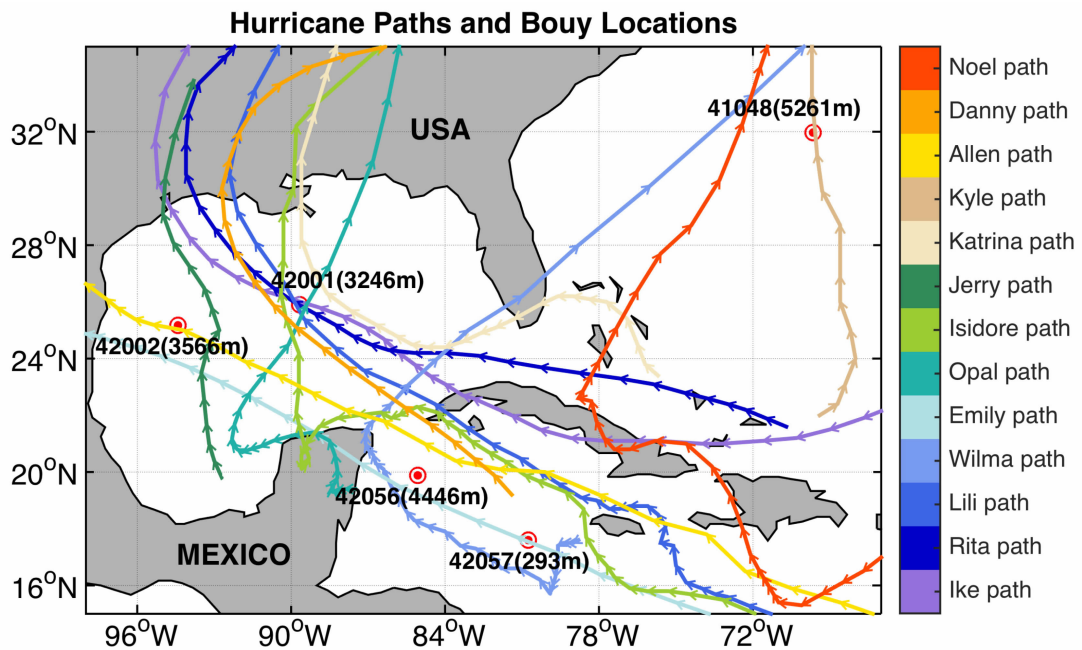


Figure 1. Buoy geographical locations and hurricane paths.

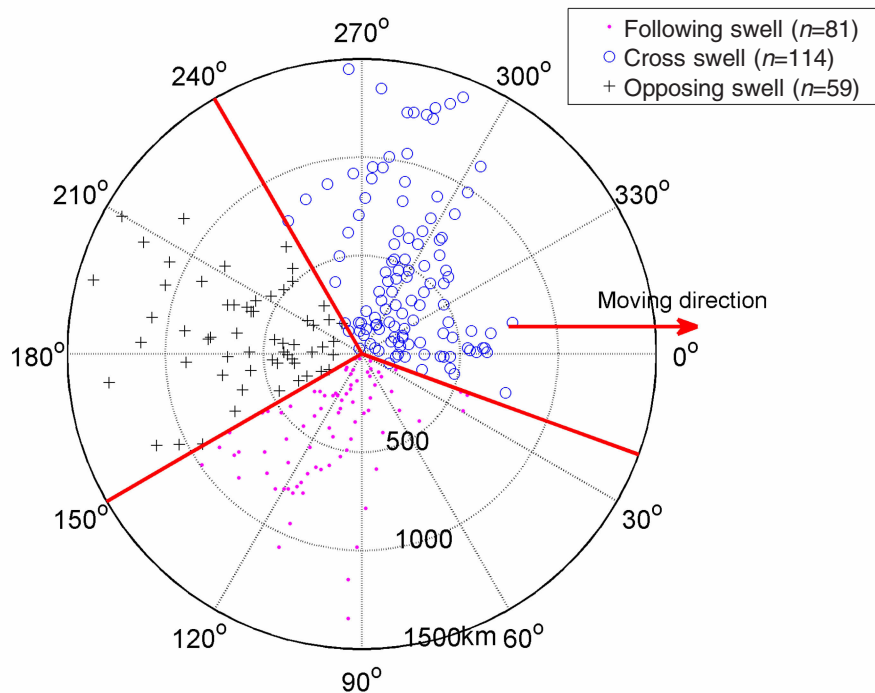


Figure 2. The distribution of swell character of the wave field and the three azimuthal sectors by Black et al.<sup>[23]</sup> and Holthuijsen et al.<sup>[26]</sup> superimposed. The red arrow signifies the moving direction of the hurricane, and the center of the circle represents the center of the hurricane.

the three swell regimes can be regressed with the equation  $H_s = a \exp(b U_{10}^{-1})$ , where  $a$  (units: m) and  $b$  (units:  $s m^{-1}$ ) are regressive coefficients, since the powers of  $U_{10}$  in three regressive equations shown in Fig. 3 are very close to  $-1$ . Fig. 4 is the same as Fig. 3, except that the regressive equations are restricted in the form  $H_s = a \exp(b U_{10}^{-1})$ . It can be seen that these regressive equations still have high

correlation coefficients ( $R$ ) and low root-mean-square errors (RMSE). The COARE (Coupled Ocean Atmosphere Response Experiment) algorithm uses  $H_s = 0.018 U_{10}^2 \times (1 + 0.015 U_{10})$  (red dash dot line) for  $H_s$  initialization (also shown in Figs. 3 and 4), which is valid under low to moderate wind speed conditions. Specifically, COARE algorithm produces an increasing

$H_s$  along with larger wind speed, but measurements shows that  $H_s$  becomes saturate when wind is larger than about  $27 \text{ m s}^{-1}$ : for the following and/or crossing swell

regimes it is 11.2 m, while for opposing swell regime it is 8.1 m (Fig. 4).

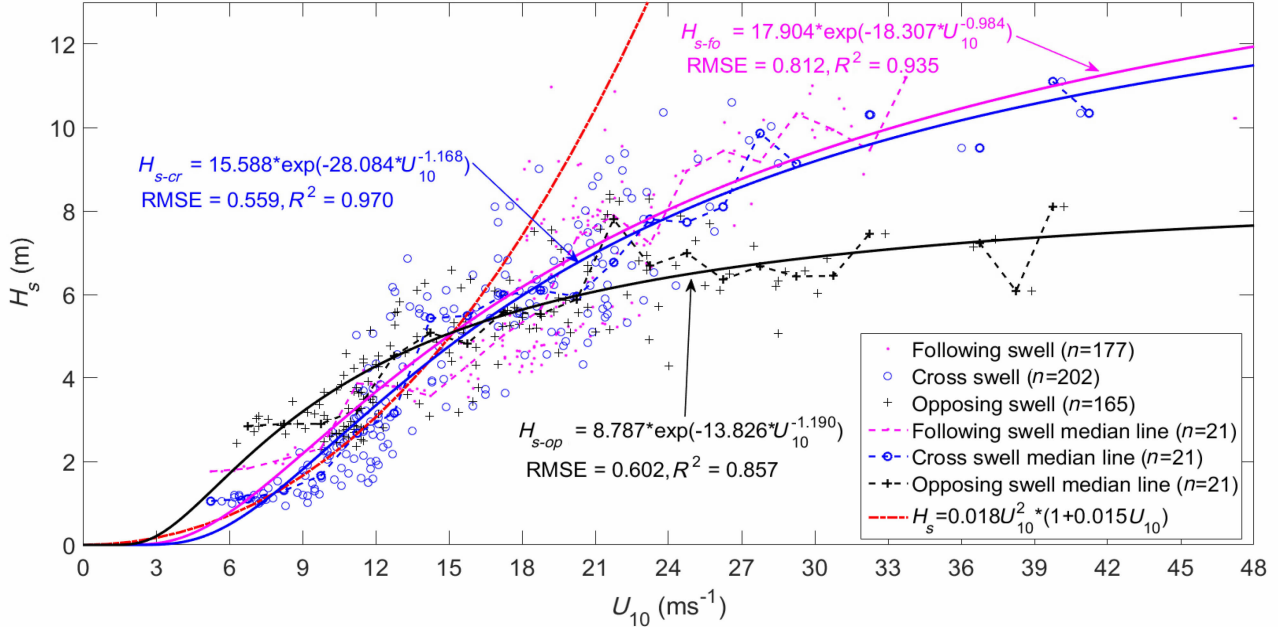


**Figure 3.** The scattered plot of significant wave height ( $H_s$ ) against 10-m wind speed ( $U_{10}$ ). The median line is for the  $U_{10}$  interval of  $3 \text{ ms}^{-1}$ .

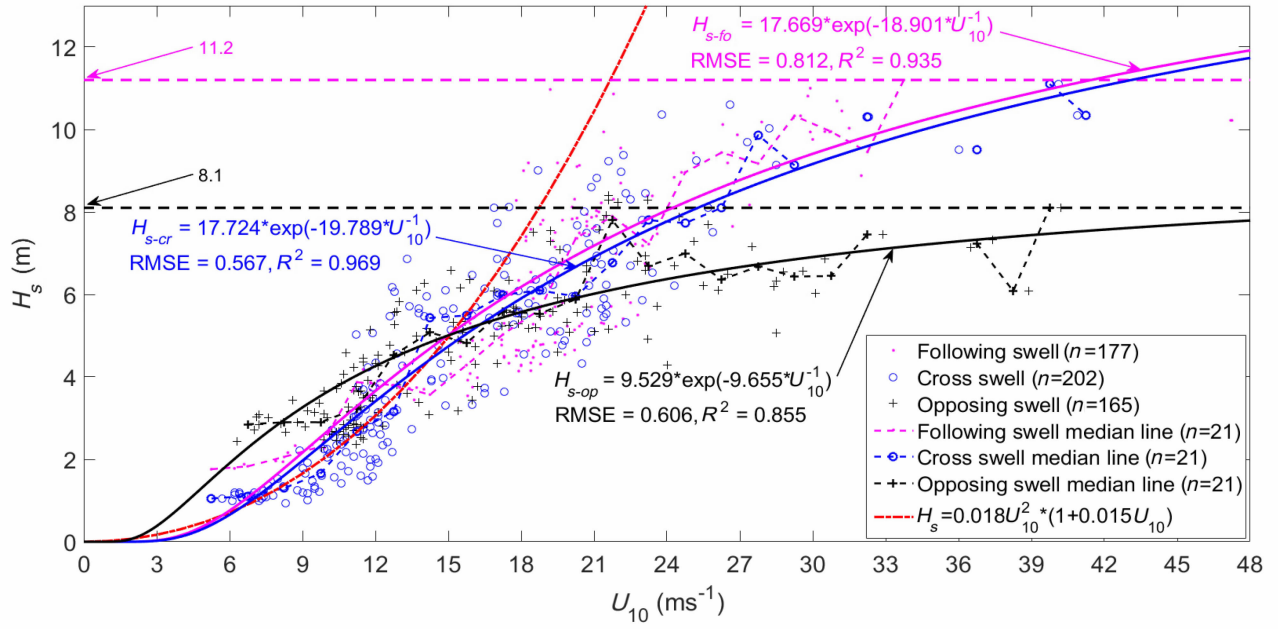


**Figure 4.** The same as Fig. 3, except that the regressive equations are restricted in the form  $H_s = a\exp(bU_{10}^{-1})$ .

By using the HEXMAX database, Gao et al.<sup>[2]</sup> validated Equations (2) and (3),

$$H_s = Bu_*^2 (2\pi c_p / u_*)^{3/2} / g, \quad (2)$$

$$u_* = 0.0353 \frac{U_{10}^{4/3}}{c_p^{1/3}}, \quad (3)$$

where  $u_*$  is the friction velocity,  $c_p$  is the phase velocity of the peak wave spectrum,  $B$  is an empirical constant (0.071), and  $g$  is the acceleration due to gravity (for which

we use  $9.81 \text{ m s}^{-2}$ ). Because there were no  $u_*$  measurements on buoy, we inserted Equation (3) into Equation (2) to eliminate  $u_*$  and plotted the relationship between  $H_s$  and  $(U_{10}^{4/3} / c_p^{1/3})^2 [2\pi c_p / (U_{10}^{4/3} / c_p^{1/3})]^{3/2} / g$  for the hurricane data in Fig. 5, and we found quadratic curves shown in Fig. 5. The curves for following swell and crossing swell are generally linear and they are very close to each other, whereas the curve for crossing swell is more parabolic than the other two.

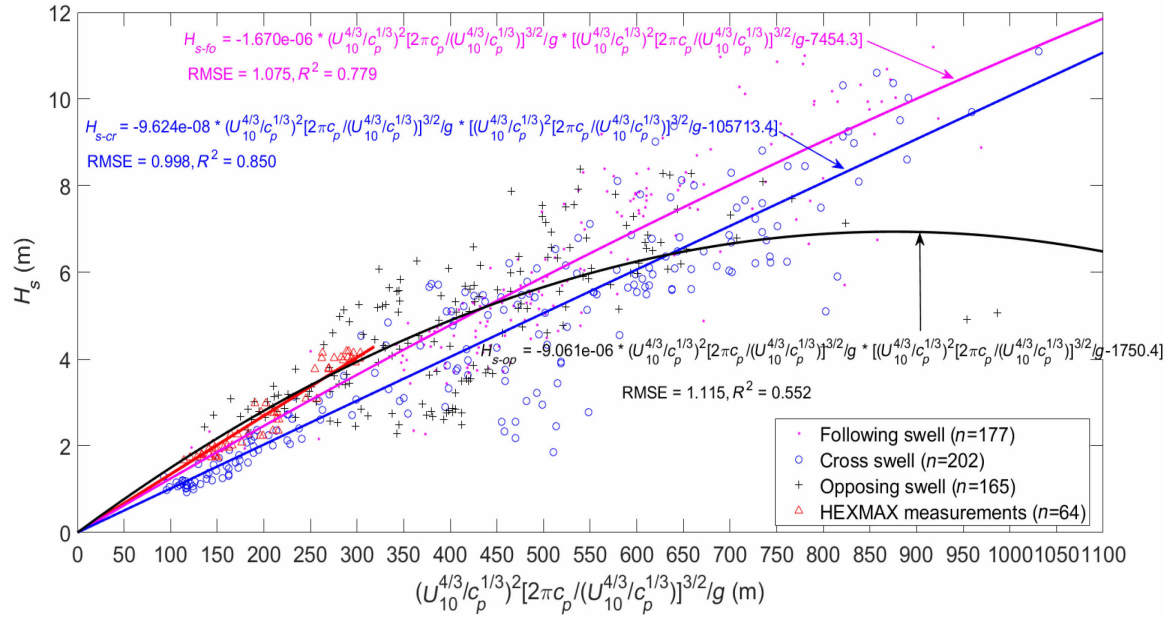


**Figure 5.** The relationship between  $H_s$  and  $(U_{10}^{4/3}/c_p^{1/3})^2 [2\pi c_p/(U_{10}^{4/3}/c_p^{1/3})]^{3/2}/g$  for the hurricane data.

### 3.2 Relationship between wave steepness ( $H_s L_p^{-1}$ ) and wave age ( $c_p U_{10}^{-1}$ )

Gao et al. [21] suggested that the wave steepness ( $H_s L_p$ ) is proportional to the  $-1/2$  power of wave age ( $c_p u_*^{-1}$ ),

$$H_s L_p^{-1} = (2\pi)^{1/2} B (c_p u_*^{-1})^{-1/2}, \quad (4)$$

where  $L_p$  is the wavelength of the waves at the peak of the wave spectrum. Since there are no direct turbulent

measurements at buoys, we have to use wave age  $c_p U_{10}^{-1}$  instead of  $c_p u_*^{-1}$ . Fig. 6 shows that wave steepness ( $H_s L_p^{-1}$ ) is proportional to the  $-2/3$  power of wave age ( $c_p U_{10}^{-1}$ ), and regressive lines of following swell (red solid line) and crossing swell (blue solid line) wind regimes are close to each other. The  $R^2$  and root-mean-square errors are also given in Fig. 6.

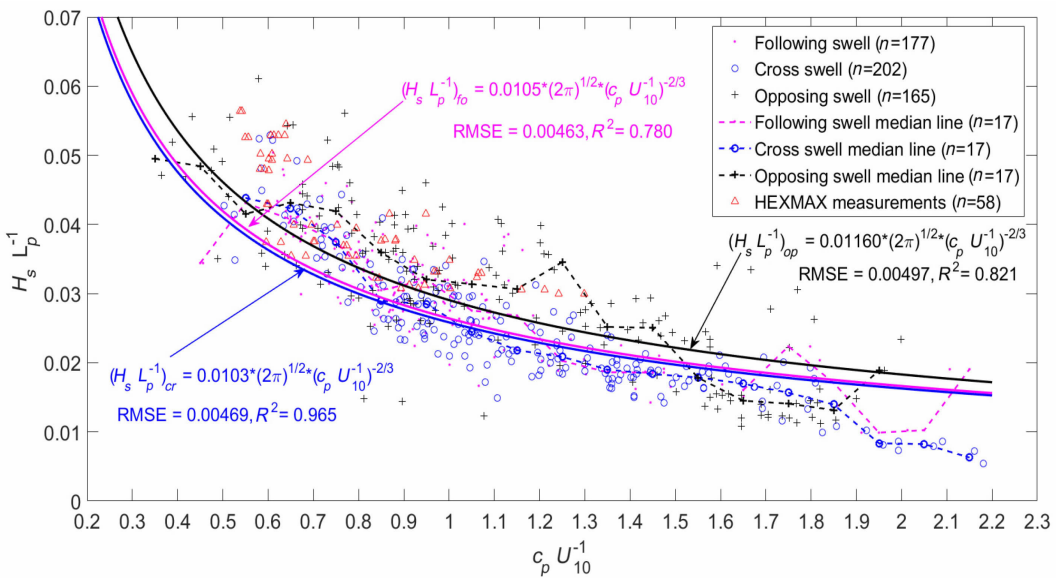


**Figure 6.** Wave steepness ( $H_s L_p^{-1}$ ) proportional to the  $-2/3$  power of wave age ( $c_p U_{10}^{-1}$ ).

### 3.3 Friction velocity $u_*$ parameterization

By using the data collected during the HEXMAX experiment, Gao et al. [22] proposed Equation (5) to calculate  $u_*$ ,

$$u_* = 0.024 U_{10} (g H_s / U_{10}^2)^{-1/4}. \quad (5)$$

We calculated  $u_*$  by applying the buoy data mentioned above into Equations (3) and (5). The

variations in  $u_*$  calculated with  $U_{10}$  are shown in Fig. 7 where the results of CBLAST (Edson et al.<sup>[27]</sup>) and in Powell et al.<sup>[28]</sup> are also given for comparison. Fig. 7 shows consistency with previous studies. We inserted the buoy data mentioned above into Equations (3) and (5) and eliminated  $U_{10}$ , which gives

$$u_* = 0.8g^2 H_s^2 C_p^{-3}. \quad (6)$$

We expect Equation (6) to help estimate  $u_*$  for the occasion where only wave parameters are available. Fig. 8 shows how the  $u_*$  estimated by Equation (6) changes with  $U_{10}$ , where the results of CBLAST (Edson et al.<sup>[27]</sup>) and in Powell et al.<sup>[28]</sup> are also shown. It is obvious that Equation (6) underestimated  $u_*$  relative to previous studies. The possible reason is that, waves can propagate

from far areas, while drag is more related to local winds.

### 3.4 Drag coefficient $C_D$ parameterization

Gao et al.<sup>[21,22]</sup> proposed Equations (7) and (8) to calculate drag coefficient  $C_D$ ,

$$C_D = 0.035(c_p/U_{10})^{-2/3}, \quad (7)$$

$$C_D = 5.76 \times 10^{-4} (gH_s/U_{10}^2)^{-1/2}. \quad (8)$$

We inserted the buoy data mentioned above into Equations (7) and (8), which gives Fig. 9, where the results of CBLAST (Edson et al.<sup>[27]</sup>) and in Powell et al.<sup>[28]</sup> are also shown. As seen in Fig. 9, compared with Equation (8), Equation (7) is more consistent with previous studies.

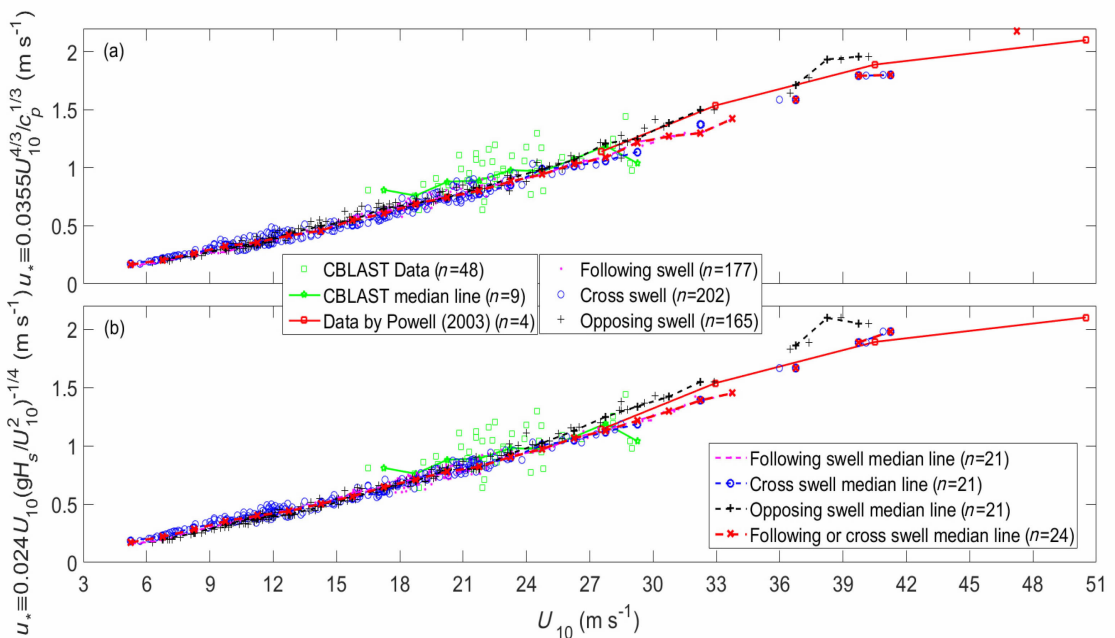


Figure 7. Variations of  $u_*$  calculated by Equations (3) and (5) against  $U_{10}$ .

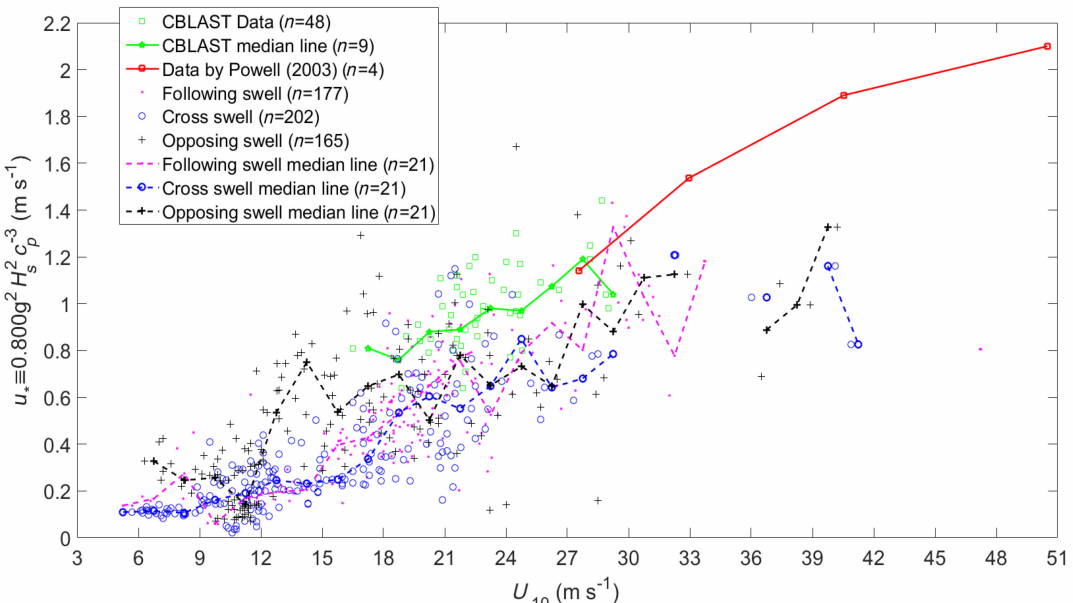


Figure 8. Variations of  $u_*$  estimated by Equation (6) against  $U_{10}$ .

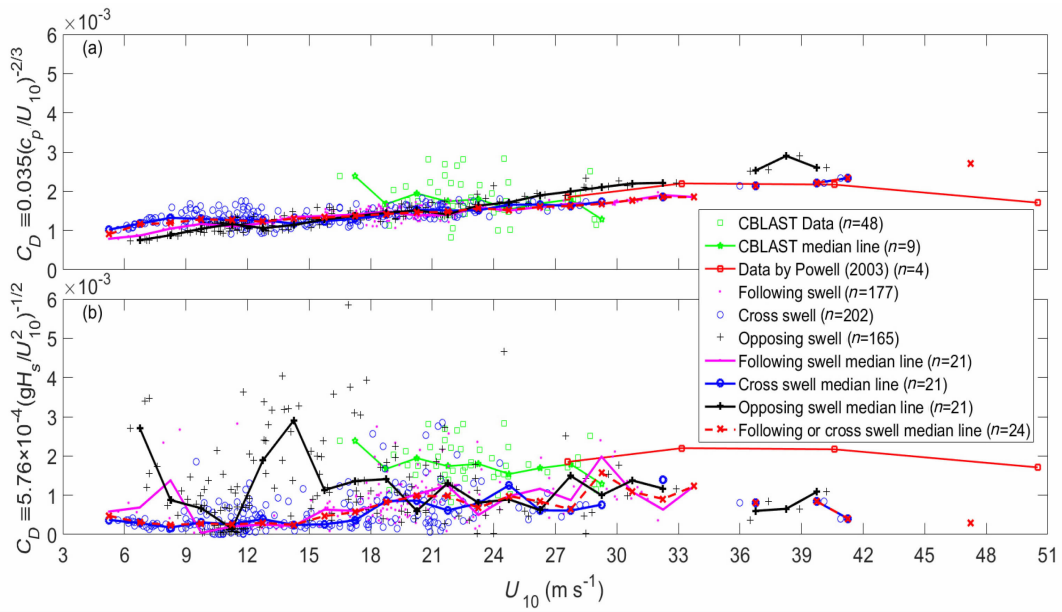


Figure 9. Variations of drag coefficient  $C_D$  against  $U_{10}$ .

#### 4 CONCLUSIONS

This manuscript describes the application of previously proposed parametric forms of integrated wave quantities and drag coefficient based on data collected from past field campaigns to wind and wave measurements from moored buoys during passage of hurricanes. Buoy data collected during 13 hurricanes are used to test wave height, friction velocity, and drag coefficient parameterizations. The results show that 1) the relationships between  $H_s$  and  $U_{10}$  are different with different wind-swell orientations. In the following swell regime and crossing swell regime, the wave height reaches the maximum value of 11.2 m when 10-m wind speed is larger than 40 m  $s^{-1}$ . However, in the opposing swell condition, the wave height is larger at low wind speed but smaller at high wind speed, compared with that in the following swell regime and crossing swell regime, and in the opposing swell conditions, the maximum wave height is saturate at 8.1 m.

2) Wave steepness ( $H_s L_p^{-1}$ ) is proportional to the  $-2/3$  power of wave age ( $c_p U_{10}^{-1}$ ), and regressive lines of following swell (red solid line) and crossing swell (blue solid line) wind regimes are close to each other, but different from that of opposing swell condition.

3) The parameterizations of friction velocity and drag coefficient with both wind and wave parameters are tested with the buoy data collected in moderate to high wind under following, crossing and opposing swell conditions, and it is found that with same 10-m wind friction velocity still can be significantly different under different wave condition.

Overall, it is suggested that wind-swell orientation

needs to be considered to retrieve accurate surface drag under high winds and strong swells, and further observation experiments need to be carried out to understand the air-sea interaction mechanism under high wind condition.

#### REFERENCES:

- [1] GREEN B W, ZHANG F. Impacts of air-sea flux parameterizations on the intensity and structure of tropical cyclones [J]. Mon Wea Rev, 2013, 141: 2308-2324.
- [2] GREEN B W, ZHANG F. Sensitivity of tropical cyclone simulations to parametric uncertainties in air-sea fluxes and implications for parameter estimation [J]. Mon Wea Rev, 2014, 142: 2290-2308.
- [3] OYAMA K. Numerical simulation of the life cycle of tropical cyclones[J]. J Atmos Sci, 1969, 26(1): 3-40.
- [4] EMANUEL, KERRY A. Sensitivity of tropical cyclones to surface exchange coefficients and a revised steady-state model incorporating eye dynamics [J]. J Atmos Sci, 1995, 52(22): 3969-3976.
- [5] ROGERS R, ABERSON S, AKSOY A, et al. NOAA'S hurricane intensity forecasting experiment: A progress report [J]. Bull Am Meteorol Soc, 2013, 94(6): 859-882.
- [6] SOLOVIEV A V, LUKAS R, DONELAN M A, et al. The air-sea interface and surface stress under tropical cyclones [J]. Sci Rep, 2014, 4, doi: 10.1038/srep05306.
- [7] PENG S, LI Y. A parabolic model of drag coefficient for storm surge simulation in the South China Sea [J]. Sci Rep, 2015, 5: 15496.
- [8] MING J, ZHANG J A. Effects of surface flux parameterization on the numerically simulated intensity and structure of Typhoon Morakot (2009) [J]. Adv Atmos Sci, 2016, 33(1): 58-72.
- [9] FRENCH J R, DRENNAN W M, ZHANG J A, et al. Turbulent fluxes in the hurricane boundary layer, Part I: Momentum flux [J]. J Atmos Sci, 2007, 64(4): 1089-1102.

- [10] JEONG D, HAUS B K, DONELAN M A. Enthalpy transfer across the air-water interface in high winds including spray [J]. *J Atmos Sci*, 2012, 69(9): 2733-2748.
- [11] DONELAN M A, HAUS B K, REUL N, et al. On the limiting aerodynamic roughness of the ocean in very strong winds [J]. *Geophys Res Lett*, 2004, 31: L18306.
- [12] BI X, GAO Z, LIU Y, et al. Observed drag coefficients in high winds in the near offshore of the South China Sea [J]. *J. Geophys Res Atmos*, 2015, 120 (13), doi: 10.1002/2015JD023172.
- [13] ANCTIL F, DONELAN M A. Air water momentum flux observations over shoaling waves [J]. *J Phys Oceanogr*, 2010, 2(7): 1344-1352.
- [14] ZACHRY B C, SCHROEDER J L, KENNEDY A B, et al. A case study of near shore drag coefficient behavior during hurricane Ike (2008) [J]. *J Appl Meteor & Climatol*, 2013, 52(9): 2139-2146.
- [15] DONELAN M A, DOBSON F W, SMITH S D, et al. On the dependence of sea surface roughness on wave development [J]. *J Phys Oceanogr*, 1993, 23 (9): 2143-2149.
- [16] YELLAND M, TAYLOR P K. Wind stress measurements from the open ocean[J]. *J. Phys Oceanogr*, 1996, 26: 541-558.
- [17] OOST W A, KOMEN G J, JACOBS C M J, et al. New evidence for a relation between wind stress and wave age from measurements during ASGAMAGE [J]. *Boundary Layer Meteorol*, 2002, 103: 409-438.
- [18] OOST W A, OOST E M. An alternative approach to the parameterization of the momentum flux over the sea [J]. *Boundary Layer Meteorol*, 2004, 113: 411-426.
- [19] GAO Z, HU W, LIU S. Test of the Louis scheme and COARE algorithm for friction velocity in different wind-sea/swell regimes [J]. *Acta Oceanol Sin*, 2005, 24 (4): 1-9.
- [20] DONELAN M A, CURCIC M, CHEN S S, et al. Modeling waves and wind stress [J]. *J Geophys Res*, 2012, 117: C00J23.
- [21] GAO Z, WANG Q, WANG S. An alternative approach to sea surface aerodynamic roughness [J]. *J Geophys Res*, 2006, 111: D22108.
- [22] GAO Z, WANG L, BI X, et al. A Simple Extension of “An alternative approach to sea surface aerodynamic roughness” by Zhiqiu Gao, Qing Wang, and Shouping Wang [J]. *J Geophys Res*, 2012, 117: D16110.
- [23] BLACK P G, D'ASARO E A, DRENNAN W M, et al. Air sea exchange in hurricanes: Synthesis of observations from the Coupled Boundary Layer Air-Sea Transfer Experiment [J]. *Bull Am Meteorol Soc*, 2007, 88 (3): 357-374.
- [24] DONELAN M A, DRENNAN W M, KATSAROS K B. The air-sea momentum flux in conditions of wind sea and swell[J]. *J Phys Oceanogr*, 1997, 27(10): 2087-2099.
- [25] SUGIHARA Y, TSUMORI H, OHGA T, et al. Variation of whitecap coverage with wave-field conditions [J]. *J Mar Syst*, 2007, 66(1-4): 47-60.
- [26] HOLTHUIJSEN L H, POWELL M D, PIETRZAK J D. Wind and waves in extreme hurricanes [J]. *J Geophys Res: Oceans*, 2012, 117(C9).
- [27] EDSON J B, JAMPANA V, WELLER R A, et al. On the exchange of momentum over the open ocean [J]. *J Phys Oceanogr*, 2013, 43(8): 1589-1610.
- [28] POWELL M D, VICKERY P J, REINHOLD T A. Reduced drag coefficient for high wind speeds in tropical cyclones [J]. *Nature*, 2003, 422(6929): 279-283.

**Citation:** PENG Wen-wu, GAO Zhi-qiu, LI Yu-bin, et al. Testing drag coefficient approaches by using the buoy data collected in moderate to high wind under following, crossing and opposing swell conditions [J]. *J Trop Meteor*, 2019, 25(3): 336-343.

Reproduced with permission of copyright owner. Further reproduction  
prohibited without permission.